*17th World Conference on Earthquake Engineering, 17WCEE*
*Sendai, Japan - September 13th to 18th 2020*

# EFFECT OF DRAWDOWN AND DENSITY ON DYNAMIC RESPONSE OF EARTHEN EMBANKMENT

G.Adapa[(1)], K.Ueda[(2)], R.Uzuoka[(3)]

[(1)] *PhD Student, Department of Civil and Environmental Engineering, Kyoto University, adapa.gautamu.48m@st.kyoto-u.ac.jp.*
[(2)] *Assistant Professor, Disaster Prevention Research Institute, Kyoto University, ueda.kyohei.2v@kyoto-u.ac.jp.*
[(3)] *Professor, Disaster Prevention Research Institute, Kyoto University, uzuoka.ryosuke.6z@kyoto-u.ac.jp.*

## *Abstract*

Earthen embankments are important geostructures which have been used by humans for a very long time. Analyzing the dynamic behavior of an embankment is important when retrofitting an existing embankment or implementing precautionary measures while constructing a new one. So, studying the behavior of an embankment during shaking when subjected to various upstream conditions would be important. In this paper, we conduct dynamic centrifuge experiments on an embankment model by controlling the water level on the upstream side of the embankment, so that we can subject it to different conditions. In this paper, we have subjected the embankment model to two different upstream conditions, in the first case we raise the water until it reaches 3/4$^{th}$ of the height of embankment on the upstream side and wait for the embankment to achieve steady state and then apply shaking. In second case, we raise the water level to 0.95 of height of embankment and wait till steady state is achieved and then drain the water to 3/4$^{th}$ the height of embankment and then apply shaking. The target shaking in this study is a wave of sinusoidal function with maximum acceleration of 300 gals. The external parameters in both the cases before shaking are same, but the only difference between both cases would be the internal degree of saturations or the saturated zone in the embankment. We made the embankment model with two unit weights of 16.2 kN/m$^3$ and 15.2 kN/m$^3$ and subject them to these conditions. We present results of pore water transducers and accelerometers placed at different points in the embankment for all the cases. A laser displacement sensor is used to measure settlement on top of the embankment and a high speed camera is used to record video of the model during shaking. Image analysis is done to track deformation of embankment after shaking using the video from the high-speed camera. We observe that, in the embankment with unit weight of 16.2 kN/m$^3$, even though pore water pressure values are not that different from each other between the two cases, the acceleration response between the two cases is different and there is no deformation in the embankment. Whereas, in the embankment with unit weight of 15.2 kN/m$^3$, the embankment has completely deformed with major displacements within the embankment and settlement at the top of embankment in both the cases, but there was a slight difference in the way the embankment was deformed between the two cases. From the results and observations done in this study we could conclude that the dynamic response of an embankment is greatly dependent on the degree of saturation at different points of the embankment before shaking and the density which could be achieved in the field.

*Keywords: Embankment; drawdown; seepage; centrifuge model; deformation.*

## 1. Introduction

Agricultural reservoirs or dams have been constructed from a long period of time to store water and use it for different purposes of humanity in the world. Storage of water in recent years, which has become difficult due to drastic climate changes everywhere in the world and scarcity of water, has been affecting most of the population in the world. Understanding the behavior of embankments is very important as they have an important role in everyone's life either directly or indirectly. Most of the earthen embankments which are still functional were mostly constructed in the times when high-tech technologies were not available and homogeneous earth fill dams comprises of 10% of the world embankments [1]. The water level in the storage of these reservoirs formed by these embankments would change and vary continuously, depending on the amount of water supplied for agricultural purposes and water accumulated in reservoirs due to rainfall in the catchment area.

Embankments are geotechnical earthen structures acting as an obstruction to the flow of water from upstream and gets subjected to seepage and capillary action with in the embankment. So, it is important to understand their behavior by considering unsaturated condition and different external influences. Many studies related to embankments were done related to centrifuge modelling with embankment on foundations to study the effects of foundation on embankment without any flow in the embankment during and after shaking [2-8]. Some studies were related to physical modelling in centrifuge considering seepage and with different materials but there wasn't any dynamic analysis [9-11].

Theoretical studies to predict the failure of embankment during earthquakes was started in 70$^{th}$ century [12], which informs us the importance given to these structures. As for the dynamic physical modelling done by Higo.et.al [13], focus was given to study the deformation of embankment for roads with different water contents. Many analytical solutions for these structures were given by many reputed researchers. But, these analyses were done by considering many assumptions. Later researches have started analyzing the earth structures by using FEM [14,15]. But, the centrifuge tests targeting the seepage and the dynamic analysis of the earthen embankment with different upstream conditions are being done recently [16,17]. Centrifuge experiments with different external influences on these type of structures are very important to analyze these structures. So, in this study we have made 4 different cases of embankments and subject them to seepage and then shaking was induced, to observe the effect of density and the water content of the soil in the unsaturated zone of the embankment on the response of the embankment.

## 2. Test method and material

### 2.1 Geotechnical centrifuge

In this study, to perform the centrifuge experiments on earthen embankment, the geotechnical centrifuge at the Disaster Prevention Research Institute (DPRI), Kyoto University was used. The effective rotation radius, defined as the length from the rotation axis of the arm to the center of the model, is 2.5±0.05m. The maximum centrifugal acceleration is 200G without shaking. If, we use shaking table the limitation for the centrifugal acceleration is 50G.

### 2.2 Model container

In this study to perform experiments, we used a custom built box with numerous parts which are shown in fig.2 with different functions to control the movement of water within the box. The movement of water is controlled remotely when the model is subjected to an acceleration field of 50G. Overhead tank is filled with water, which is the main source for the whole experiment, before the box is subjected to centrifugal acceleration. Reservoir valve is the only valve to operate and control the flow of water from overhead tank into the box. Once the reservoir valve is opened by using a remote control during the centrifugal rotation, water starts flowing from overhead tank into intermediate compartment. Electrodes are inserted inside the intermediate compartment to automatically maintain the water input. Then the water passes through a supply valve, which is set before the box is set into flight as it can only be operated manually, into the embankment model. Slits for drainage on both sides of the box are connected to Drainage tank through drainage valve. These slits allow the water from the chamber into the drainage tank and can be controlled remotely during flight in centrifuge.

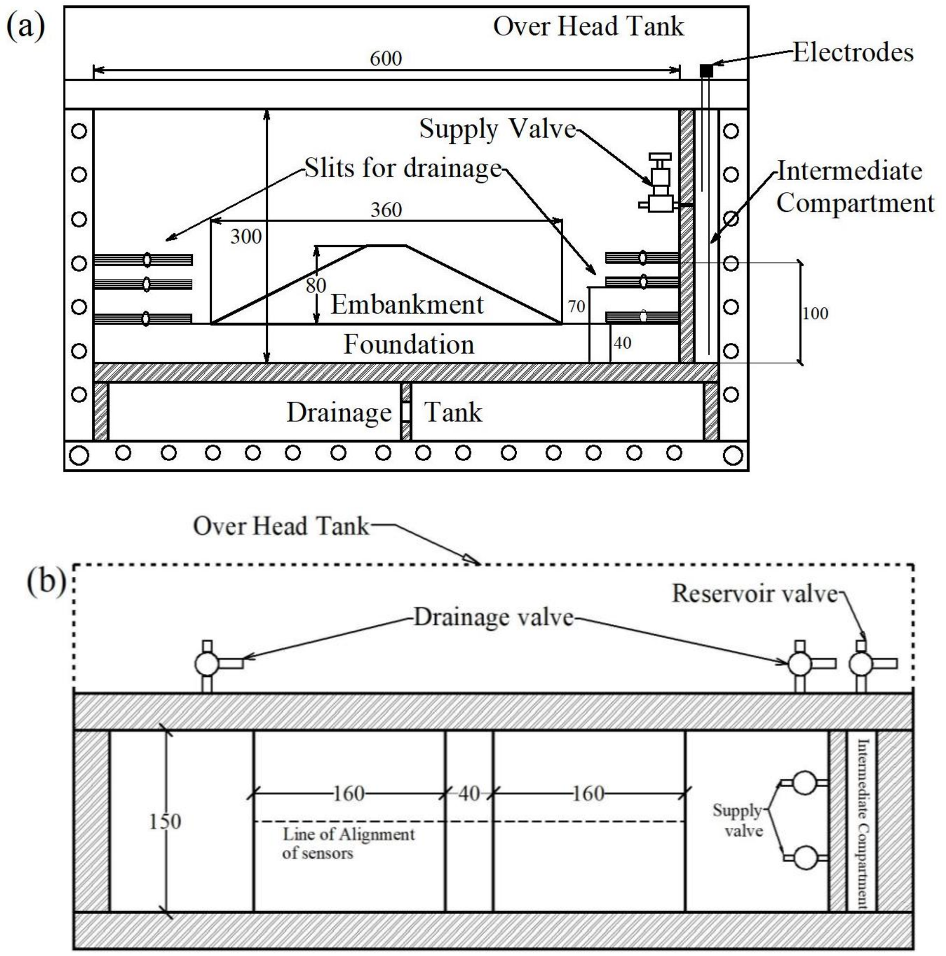


Fig. 1 – Container used in this study a) front view b) top view (units:mm)

## 2.3 Material

### 2.3.1 Embankment

We used Masado as the material for the embankment as it is the most found soil in Japan used for construction of geotechnical structures. Fig.2 shows the grain size distribution of the Masado soil used in the experiments. Maximum dry density and optimum moisture content for the Masado soil were obtained using 2kg rammer compaction test, observed in Fig. 3. Properties of the soil are shown in table. 1.

### 2.3.2 Foundation

For the foundation of the embankment, we have considered to use an impermeable rigid foundation, so to focus on the dynamic behavior and seepage of the embankment. So, we have used foundation made of cement mortar which could replicate both rigid and impermeable behavior during the experiment.

### 2.3.3 Fluid medium

The fluid medium used in model to represent water in prototype scale was water, instead of a higher viscous fluid. Steady state within the embankment is achieved by allowing the fluid to flow from upstream side to downstream side. Using higher viscous fluid would result in decrease in permeability and achieving steady state within the embankment during centrifugal rotation would take much longer time. This is not feasible and hence, water was used as the medium for fluid to achieve steady state in embankment within a limited time in model scale. Using water as a medium would usually take almost 2 hours in centrifugal flight at 50G to perform one experiment.

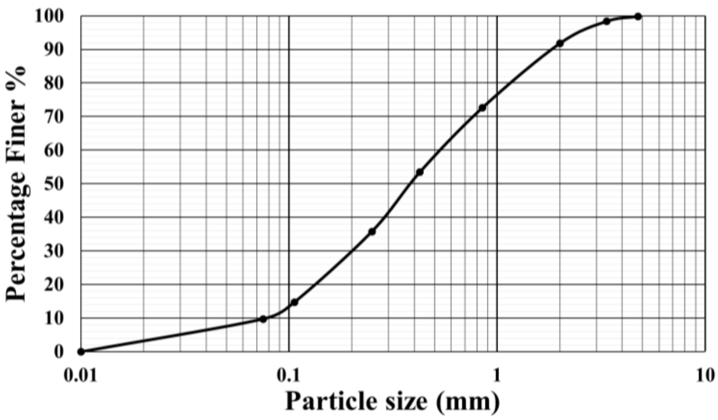


Fig. 2 – Grain size distribution curve for Masado soil

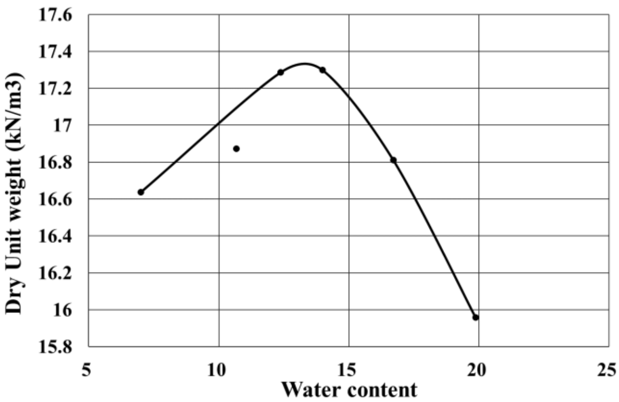


Fig. 3 – Compaction curve of Masado soil

Table 1 – Material properties of Masado soil used in this study

| | |
|---|---|
| Sand (%) | 90.23 |
| Silt (%) | 9.77 |
| Maximum particle diameter (mm) | 4.75 |
| Average particle diameter (mm) | 0.38 |
| Specific Gravity of soil G | 2.6 |
| Minimum Void ratio $e_{min}$ | 0.465 |
| Optimum moisture content $w_{opt}$ (%) | 14.3 |
| Maximum dry unit weight $r_{dmax}$ (kN/m$^3$) | 17.35 |
| Permeability of soil at 95% DOC $k$ (m/sec) | $1.6\times10^{-7}$ |



 

### 2.4 Model preparation

The height of embankment is 8cm, width of crest is 4cm and the slope of both upstream and downstream is 2H:1V. This embankment model rests on a solid foundation and impermeable in nature. This study is not only focused on the dynamic nature of the embankment but also the static analysis of seepage within embankment. Impermeable foundation is used in this study, so that the nature of foundation would not affect the seepage within the embankment for the static analysis. Whereas, in dynamic analysis we would need a rigid foundation as for the shaking to directly transfer into the embankment without any deformation in the foundation. These disturbances are avoided by using a rigid and impermeable foundation.

For preparing the embankment in the box, we have used compaction method as the soil material is silty sand. So, we have calculated the amount of soil required to compact and add 12% by weight of water and mix them to make a uniform mixture and place them in layers of 2cm of height each and compact each layer to achieve the target density, as shown in fig.4(a). Sensors are placed in the first layer and third layers only and these are placed before the soil is compacted at required locations. After completing compaction, the model would look like steps as shown in fig.4(a) and tool is used scrape the soil to achieve the required slope we intend to. So that, we would finally achieve a symmetrical embankment with a 2H:1V slope.

Pore water pressure (PWP) transducers with porous stone filters are used to measure the water pressure. Accelerometer transducers are used to observe the response of embankment during shaking and these are placed at the middle of the container along a dotted line, as shown in fig.1(b), as the response of the sensors are much efficient at that location. Fig. 4(b) shows the placement and the notations of the sensors used in this study of pore water pressure transducers and accelerometers. A laser displacement sensor is used to measure the settlement of the crest of the embankment during shaking. Image analysis is also used in this study to trace the deformation of embankment caused by shaking, from the video which is captured using a high speed camera within the centrifuge.

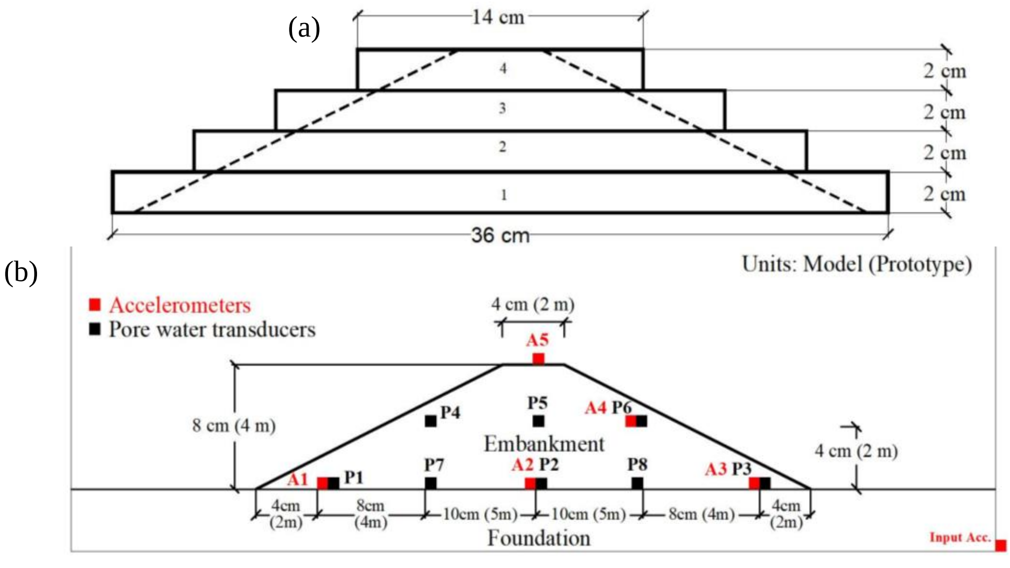


Fig. 4 – Model set up a) Schematic view of the model before scraping. b) Cross-section view of model with sensors placement

## 3. Testing program

### 3.1 Test cases

Two different cases done in this study are shown in Table 2 with two dry unit weight of the embankment. In this study, after the model is fixed inside the centrifuge, we wait till the centrifugal acceleration achieves 50G. After that, in Case 1, we maintain the water on the upstream side of the embankment at 3m, as shown in fig.5. Whereas, in Case 2, initially the water level is raised to 3.75m and let the water flow through embankment until a steady state is achieved then the water level is drawn to 3m, as shown in fig.5. These cases are done on embankments with two different average dry unit weights of 16.2 and 15.2 kN/m$^3$.

Table 2 – Test cases done in this study

| **Cases** | | **Average dry unit weight** | **Upstream condition of the embankment** |
|---|---|---|---|
| Case1 | a | 16.2 kN/m$^3$ | Maximum of 3m water level |
| | b | 15.2 kN/m$^3$ | |
| Case 2 | a | 16.2 kN/m$^3$ | 3.75m to 3m drawdown |
| | b | 15.2 kN/m$^3$ | |

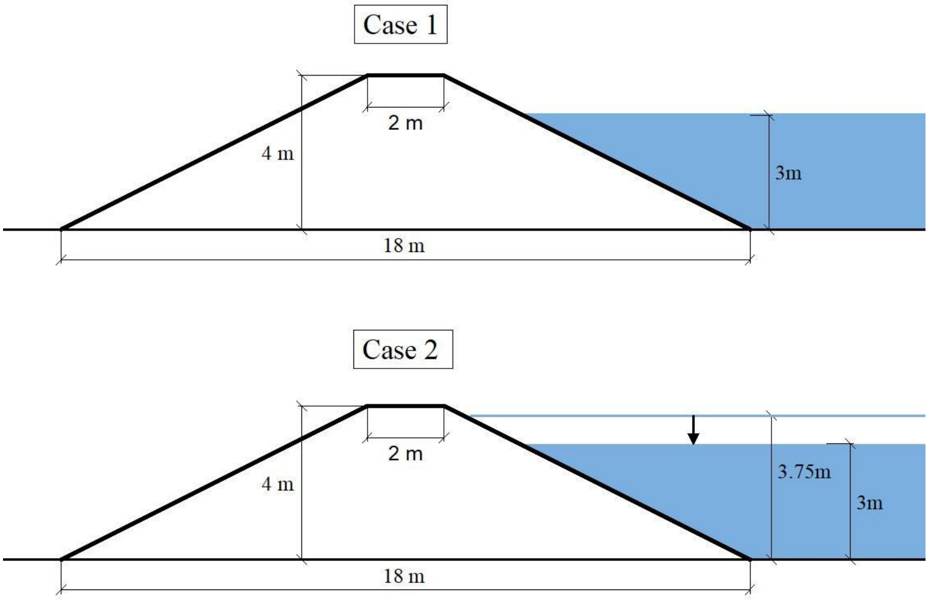


Fig. 5 – Schematic view of embankment for the cases

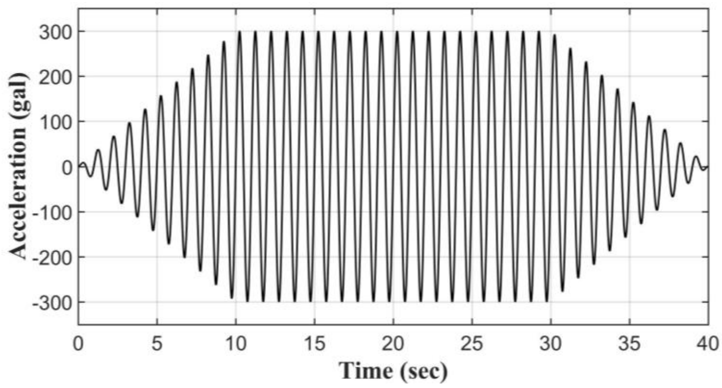


Fig. 6 – Target input acceleration time history in all cases

3.2 Testing procedure

The model embankment is prepared by compaction method in layers to achieve the target density. During the construction of embankment, measuring instruments are placed at the prescribed locations, as shown in fig.4(b). Four accelerometers and eight pore water pressures are embedded in the embankment. Then the model shown in fig.4(a) is formed and then the extra soil is scarped and formed into embankment. One accelerometer is placed on top of the embankment and laser is placed to measure the vertical displacement of the top of embankment.

Then the model container is mounted on the shaking table of the centrifuge machine and the centrifugal acceleration is gradually increased up to 50G spending about 15 min in model scale. After that, the embankment is subjected whatever condition we want is done like cases shown before. During this process of achieving steady state the readings are recorded every second in model scale. This process usually takes 45 to 60 min in model scale. Then, once the static process of steady state is done, the frequency for sampling data is change to 0.2ms in model scale for the shaking. Then the shaking is given to the model through the shaking table.

### 3.3 Input motion

In all the cases in this study, a tapered sinusoidal wave with a frequency of 1 Hz (50 Hz in model scale) is used. The duration of the input wave is 40 secs (0.8 sec in model). The target amplitude for the model is 300 gals. The shaking table in the centrifuge takes the displacement time history as the input file and the acceleration induced in horizontal direction is measured by accelerometer attached on top of shaking table. The target input wave for all the cases in this study is shown in fig.6.

## 4. Results

In this study results of the experiment during seepage and shaking of the model are shown. The influence of density and pore water pressures on the behavior of the embankment will be discussed in detail in this section.

### 4.1 Seepage

During seepage in the embankment, the water on the upstream side travels through the embankment on to the downstream side as the embankment is a permeable structure. In the centrifuge tests of the cases shown in table-2, data from all the pore water transducers installed inside embankment are sampled at a frequency of 1Hz in model scale. The parameters which effect the values of pore water pressure are dry unit weight of the embankment and the level of water in the reservoir.

The height at which the pore water transducers are placed is 0m and 2m, the sensors at 2m would be the ones closer to the water level within in the embankment. So, to know the distribution of water in the embankment, it would be better to see the values of sensors at 2m and the one sensor ‘P1’ at the toe end.

In Case 1, the sensor close to the top surface of water on upstream side is P6 and the value of P4 is zero in both cases Case 1a and Case 1b. The values of P1, P5 and P6 of Case 1a and Case 1b can be seen in fig.7(a). It could clearly be seen that even though the value of P6 which represents the height of water surface is almost same for Case 1a and 1b, the values of P1 and P5 are nowhere near to each other. This difference between the cases Case 1a and 1b is because of the difference in their dry unit weights.

The effect of dry unit weights on the behavior of embankment is demonstrated much better in Case 2. In Case 2, the sensor to represent the water surface on upstream is P5, because it is almost below the surface when the height of water level is 3.75m in prototype scale. We could observe a reduction of the value of P1 value in Case 2b because of damage to the embankment at the toe of embankment. This damage of the embankment during seepage is shown in fig.8.Also in Case 2 after draining and reducing the water level to 3m, we could observe a quick change in the values of P4 of Case 2b but not Case 2a.

We could also observe that in fig.7(b) that in Case 1a and 2a there is a huge difference in time for the P1 value to start increase in its value but in Case 1b and 2b the value of P1 increase at the same time. Also, time is also an important element which gets influenced easily by the variations in the parameters of dry unit weight and upstream water level, as shown in fig.7.



 

From the fig.7, we can conclude that the time taken for the embankment to reach steady is affected greatly by the upstream water level than the density of the embankment. Piping has occurred during the seepage through the embankment on downstream slope only in Case 2b which has higher water level initially than Case 1b even though they have the same density.

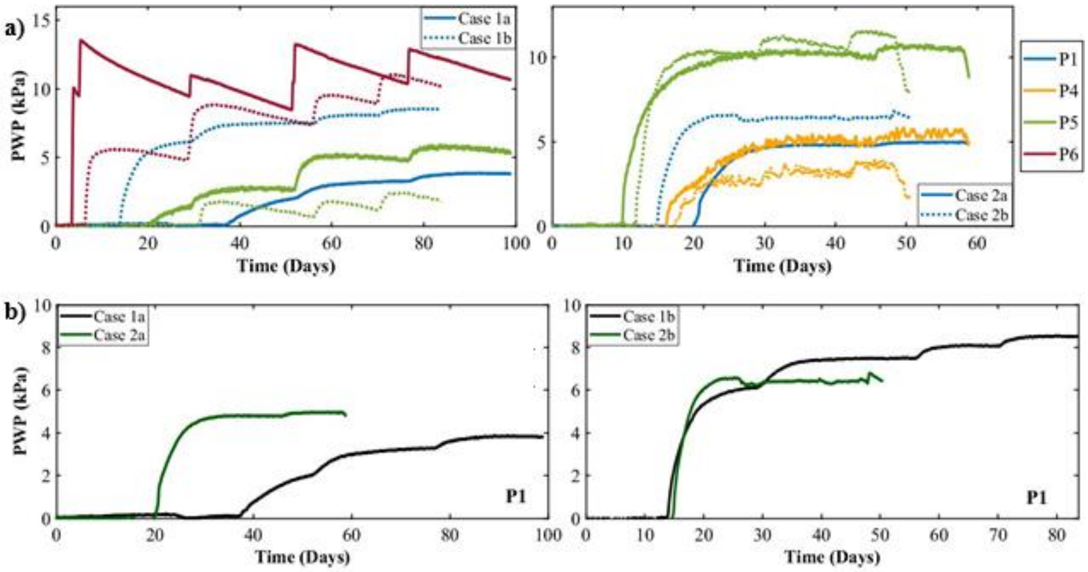


Fig. 7 – Values of pore water pressure during seepage in the embankment.

Fig. 8 – Top view of the damage to the embankment at downstream side in Case 2b during seepage.

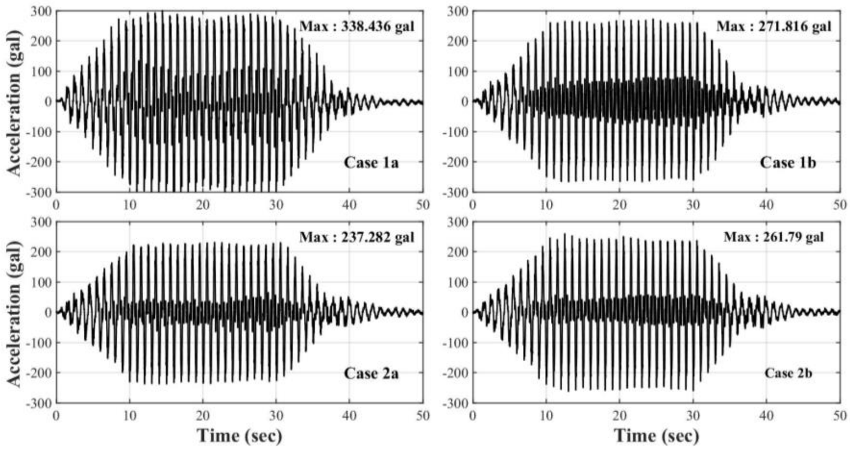


Fig. 9 – Response of Input Acc. placed at the top of shaking table.



 

### 4.2 Shaking

In this study, after the embankment is subjected to the seepage, shaking was given to the model. The horizontal acceleration given to the box and the maximum acceleration in all cases is shown in fig.9. In this section, the influence of unit weight and pore water pressure on the behavior of embankment during shaking will be scrupulously validated using results from accelerometers, pore water pressures and image analysis of the embankment.

#### 4.2.1 Pore Water Pressure

There is a difference in time of recording the data from seepage and shaking, because we need to change the frequency of recording. The difference in recording the data is around 5 minutes in model scale. So, to know the effect of pore water pressure on response of the embankment, pore water pressure values before the shaking is given to the model are plotted and shown in fig.10.

In Case 1a, P7 and P8 were not recorded. The sensors were placed inside embankment with the notations as shown in fig.4b. In fig.10 we could observe that the value of P3 is almost same in all cases which represents the water level on upstream side of embankment. The pore water pressure at all the positions in Case 1b is little lower than other cases except at P1. At P4, Case 1a and 1b had shown zero, but in Case 2a and 2b the value is higher than zero. Overall, the major difference could only be seen in Case 1b than the other cases. The results show that the pore water pressure values in the embankment are almost same before shaking even though each case has either a different upstream water level or different density.

#### 4.2.2 Deformation of Embankment.

In cases, Case 1a and 2a, there is no deformation to the embankment in anyway. Only in cases, Case 1b and 2b, embankment has deformed which was tracked using an image analysis software analyzing the movement from the video recorded using high speed camera. Even though there isn't much difference in pore water pressures, the deformation and the vertical settlement of the embankment between the cases is contrasting. The deformation and the displacement vectors of Case 1b shown in fig.11a is contrasting to Case 2b shown in fig.11b. Deformation of embankment in Case 1b is more symmetrical but in Case 2b deformation is more towards the downstream side which could be observed by the displacement vectors.

The vertical settlement measured using LVDT of Case 1b is 290 mm and of Case 2b is 220 mm in prototype scale. The embankment of higher density had no deformation. Whereas, the embankments of lower density were deformed hugely and the displacements tracked using image analysis on the video from high-speed camera suggests us that the deformation is even dependent on the water content within the embankment

#### 4.2.3 Maximum Horizontal Acceleration

Acceleration response of the sensors in horizontal direction was recorded. In fig.12 the maximum acceleration at the specified location as shown in fig.4b of all the cases done in this study are shown. In Case 1b as the embankment was deformed the sensors were also displaced at locations A1, A2 and A3. In Case 2b, sensors placed at A1 and A3 are displaced and hence those high values than that of Case 2a. Form fig.12, we should observe the cases Case 1a and 2a, as the embankment was not deformed and yet a complete different response of accelerometers were observed even though the input wave is similar in both cases as shown in fig.9. Comparing Case 1a and 2a, the only difference between the cases is only the water content of soil in the embankment as the water level was reduced to 3m from 3.75m and yet the maximum acceleration of the accelerometers response is contradictory between the two cases in fig.12.

The results from maximum acceleration of acceleration responses at different points in embankment of all the case from this study shows that the response of embankment to shaking is affected by density to which the embankment is compacted and also by the distribution of water content within the embankment.


 

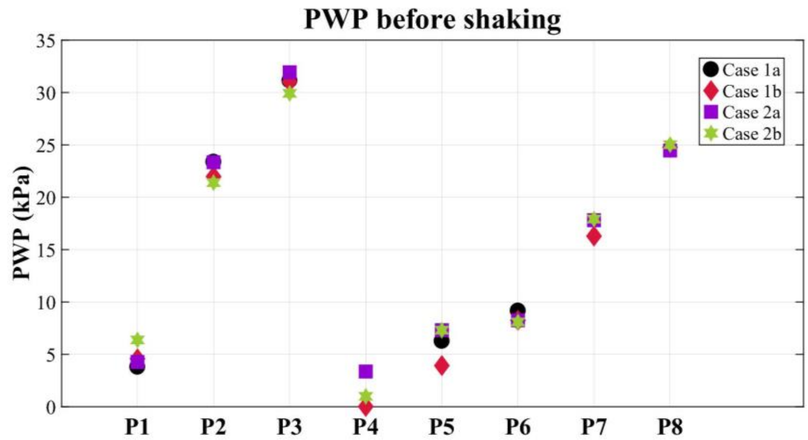


Fig. 10 – Pore water pressure values of all cases before shaking was induced

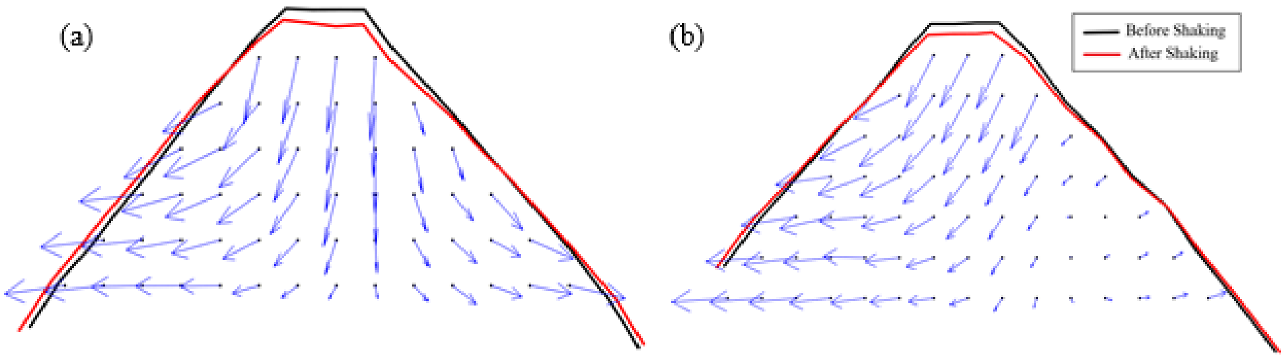


Fig. 11 – Deformation of embankment tracked using image analysis. a) Case 1b b) Case 2b

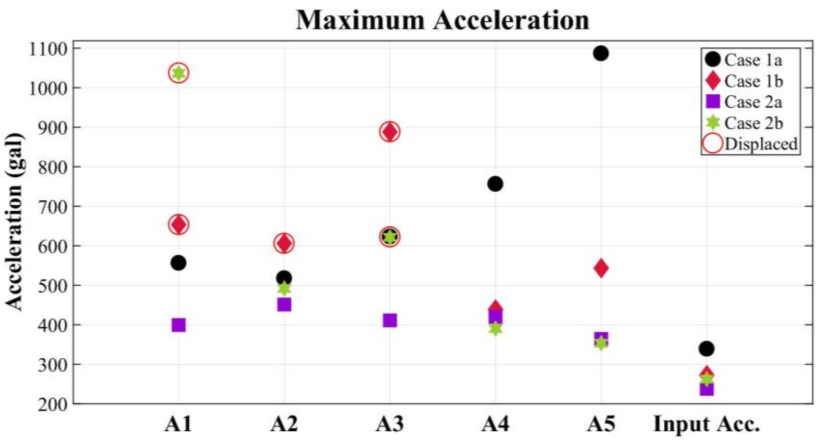


Fig. 12 – Maximum acceleration recorded at different positions in all the cases done in this study.

## 5. Conclusions

Dynamic centrifuge experiments on embankment with two different densities and different unsaturated condition of the soil have been carried out. At first, water at upstream side is maintained at two different specific levels in different cases until a steady state flow is achieved in the embankment. Then the water level is brought back to the same level in all cases before shaking is induced.



 

From this study, results of both seepage and the response to shaking are observed. The conclusions made from this study are:

1) The time taken for the pore water pressure values to come to a constant value in Case 1 is higher than Case 2. This suggests that, irrespective of the density of the embankment, the time to achieve steady state in embankment is mainly dependent on the upstream water level during seepage. In addition, these results of pore water pressure also show that the effect of density is not as influential as upstream water level.

2) Piping in an embankment has occurred during the seepage through the embankment on downstream slope only in a case, in which the density is low and the upstream water level is at maintained at its highest capacity.

3) Pore water pressures in the embankment before shaking are almost similar to each other in all cases irrespective of the seepage process.

4) There is no deformation to the embankment of higher density irrespective of the upstream water level during shaking.

5) Whereas, the embankment with lower density is subjected to deformation during shaking which was tracked using a high-speed camera. The deformation of cases 1b and 2b presented using image analysis shows a different direction of displacement within the embankment. This suggests that the deformation of embankment is affected due to the distribution of water content.

6) The maximum acceleration at different points in the embankment is different in all cases even though pore water pressure values are almost similar in all the cases. The maximum acceleration on top of embankment when compared between the cases of higher density (Case 1a and 2a), shows that the embankment is stiffer to shaking in Case 1a than in Case 2a.

## 6. Acknowledgements

I would like to acknowledge the help from the technical staff of centrifuge facility of Kyoto University (Ms. Namigishi Ayako) in performing the centrifuge experiments. This research was supported by the JSPS KAKENHI (Grant-un-aid for Scientific Research grant no 18H03967).

## 7. References

[1] Foster, M., Fell, R., Spannagle, M., 2000. The statistics of embankment dam failures and accidents. Can. Geotech. J. 37, 1000-1024.

[2] Egawa. T., Nishimoto, S., Tomisawa, K., 2004. An experimental study on the seismic behavior of embankments on peaty soft ground through centrifuge model tests. 13th World Conference on Earthquake Engineering.

[3] Maharajan, M., Takahashi, A., 2014. Liquefaction-induced deformation of earthen embankments on non-homogeneous soil deposits under sequential ground motions. Soil Dynamics and Earthquake Engineering 66, 113-124.

[4] Oka, F., Tsai, P., Kimoto, S., and Kato, R. (2012). Damage patterns of river embankments due to the 2011 off the Pacific Coast of Tohoku Earthquake and a numerical modeling of the deformation of river embankments with a clayey subsoil layer. Soils Found., 52(5), 890–909.

[5] Okamura, M., Matsuo, O., 2002. Effects of remedial measures for mitigating embankment settlement due to foundation liquefaction. International Journal of Physical Modelling in Geotechnics 2 (2), 1–12.

[6] Okamura, M., Tamamura, S., 2011. Seismic stability of embankment on soft soil deposit. Int. J. Phys. Modell. Geotech. 11 (2), 50–57.

[7] Okamura, M., Tamamura, S., Yamamoto, R., 2013. Seismic stability of embankments subjected to pre-deformation due to foundation consolidation. Soils Found. 53 (1), 11–22.

[8] Rapti, I., Caballero, L.F., Razavi, M.F.A., Foucault, A., Voldoire, F., 2018. Liquefaction analysis and damage evaluation of embankment-type structures. Acta Geotechnica 13, 1041-1059.



 

[9] Bekket, C., Fourie, B.A., O'Loughlin, D.C., 2016. Centrifuge modelling of seepage through tailings embankments. Int. J. Phys. Modell. In Geotech. 16 (1), 18-30.
[10] Das, A., Jayashree, Ch., Viswanadham, B.V.S., 2009. Effect of randomly distributed geofibres on the pipng behaviour of embankments constructed with fly ash as a fill material. Geotextiles and Geomembranes 27, 341–349.
[11] Thorel, L., Ferber, V., Caicedo, B., Khokhar, I.M.,2013. Physical modelling of wetting-induced collapse in embankment base. Géotechnique 61 (5), 409–420.
[12] Newmark, N. M. (1965). Effects of earthquakes on dams and embankments. Geotechnique, 15 (2), 139–159.
[13] Higo, Y., Lee, C., Doi, T., Kinugawa, T., Kimura, M., Kimoto, S., Oka, F., 2015. Study of dynamic stability of unsaturated embankments with different water contents by centrifugal model tests. Soils and Foundations 55 (1), 112-126.
[14] Ozkan M Y. A review of considerations on seismic safety of embankments and earth and rock-fill dams. Soil Dynamics and Earthquake Engineering, 1998, 17 (7–8): 439–458.
[15] Aydingun O, Adalier K. Numerical analysis of seismically induced liquefaction in earth embankment foundations, part I. Benchmark model. Canadian Geotechnical Journal, 2003, 40 (4): 753–765.
[16] Adapa, G., Takada, Y., Ueda, K., Uzuoka, R., 2019. Dynamic centrifuge model tests on embankment with different upstream conditions. JGS special publication, 7th Asia-Pacific Conference on Unsaturated Soils (AP-UNSAT2019).
[17] Wu, C., Ni, C., Ko, H., 2009. Seismic response of an earth dam: finite element coupling analysis and validation from centrifuge tests. Journal of Rock Mechanics and Geotechnical Engineering 1 (1), 56-70.



 